Computer Assisted Mechanics and Engineering Sciences, **13**: 39–51, 2006.

Application of discrete wavelet transformation in damage detection. Part II: Heat transfer experiments

Krzysztof Ziopaja, Zbigniew Pozorski, Andrzej Garstecki
Institute of Structural Engineering, Poznań University of Technology
ul. Piotrowo 5, 60-965 Poznań, Poland

(Received in the final form February 15, 2006)

A non-destructive method of damage detection based on heat transfer experiments and 2-D Discrete Wavelet Transform (DWT) is discussed. In this paper real experiments with the use of thermography measurement techniques are substituted by numerically simulated experiments. The plates were modeled as 2-D and 3-D structures. Two kinds of structures are considered: homogeneous in undamaged state and non-homogenous. Measurement errors are accounted for by introduction of a white noise. The efficiency of the method is demonstrated by the way of numerous examples.

Keywords: damage detection, wavelet transformation, infrared thermography

1. Introduction

Structural health monitoring and early damage identification allow to increase safety and serviceability of structures. Therefore, methods of defect identification and monitoring techniques are still developed. Non-destructive techniques like thermography are in special interest. The method of damage identification based on thermal processes, when structural response is recorded by the way of thermography and compared with numerical results obtained from FEM and sensitivity analysis of the model structure was proposed in [4, 11, 12]. In an alternative approach, namely in a non-model based approach, one determines direct changes in the thermography output signal to locate damage in the structure. The major advantage of non-model based schemes is that the errors caused by model inaccuracy due to imprecise boundary conditions, details of mechanical or thermal excitation and environmental conditions can be avoided. The structural response measured in experiments is usually analyzed employing signal processing techniques. One of the most promising tools of signal analysis is wavelet transform. In papers [5, 9] the application of wavelet transform of thermography response signals was discussed. In [13] and [15] the efficiency of Discrete Wavelet Transform (DWT) in damage detection was studied basing on numerically simulated heat transfer experiments. The present paper further develops the study by consideration of different types of thermal boundary conditions, different shapes of structures and allowing for non-homogenous material. At this stage of the study computer simulated heat transfer experiments will be used and thus obtained temperature field at the surface of the structure will be subjected to the two dimensional DWT with the aim to detect and localize the defect in structures. The next Section contains concise description of the traditional approaches in non-destructive evaluation of defects by means of thermography. In Section 3 the heat transfer problem will be formulated and the background of 2D DWT will be described. Section 4 presents a series of examples of damage detection in plates. Concluding remarks are formulated in Section 4.

2. Basis of thermography

A wide and still increasing field of application of infrared thermography to nondestructive damage detection has been observed. The strengths of thermography are: no contact with the investigated specimen, fast inspection rate, portable hardware and large area inspection. The field of applications of thermography is wide: civil engineering, different industrial branches, military and medicine. In all specific applications, detection of a local variation in the temperature field can be used as a signal of an abnormal situation, which has to be analyzed individually. Thermal sensitivity of modern thermography cameras is 0.02°C [16]. Two schemes of thermography are observed: the passive approach and the active approach. Passive approach can be used when the investigated regions of material or structure in their natural states have variable temperatures as a result of special material state or feature. Practical engineering applications of passive thermography to investigation and diagnosis of buildings and reinforced concrete and stone bridges have been reported in [3, 14]. In active thermography an exterior stimulus is required to induce the variation of temperature in the tested specimen. Usually the specimen is heated, however, cooling is used, too. Various heat sources can be used. Flash lamps, laser lamps or infrared radiators can produce a single heat impulse or a series of impulses with precisely prescribed duration from [ns] to a few [s]. There can be a point, line or surface action of such heat impulse. Depending on the thickness of the specimen and on material constants, the heat transmission or heat reflection phenomena can be used in active thermography. Then, the heat source and the thermography camera are at the opposite sides of the specimen, or at the same side, respectively. Specific techniques of active thermography have been developed: pulse thermography (PT), lockin thermography (LT), pulsed phase thermography (PPT). Introduction to nondestructive testing of materials damage detection by active thermography is presented in [8].

2.1. Pulse thermography (PT)

Pulse thermography (PT), consists in a brief heating of the specimen and next in measuring the decay of temperature. In the place of defect a reflection of the heat wave, resulting in a non-uniform cooling of the material in this region is observed. A series of thermograms is registered. They allow to evaluate the thermal contrast coefficient and hence to localize the damage. In [1, 2] the results of damage detection in aircraft composites are presented.

2.2. Lockin thermography (LT)

Lockin thermography (LT), is a technique basing on the periodic sine heat stimulus, which induces the sine thermal wave within the specimen. The temperature field is measured in the stationary mode. From the thermograms we obtain phase images associated with the propagation time and amplitude images associated with thermal diffusivity. It is worth to emphasize, that by proper modulation of frequency one can obtain expected depth of penetration into the specimen. Advantages and disadvantages of using LT versus PT in damage detection in glass-epoxy laminates were presented in [6].

2.3. Pulsed phase thermography (PPT)

Pulsed phase thermography (PPT) is a signal processing technique, which is a compilation of PT and LT. The specimen is heated pulse-wise, similarly as in PT. Hence, thermal waves with variable frequency and amplitude can be induced within the specimen. The phase and amplitude images are obtained similarly as in LT. The difference is that real and imaginary parts are extracted from each pixel of the temperature field using one dimensional discrete Fourier transform. Paper [7] provides a concise description of thermography investigation and incidentally the application of

Fourier transform or optionally wavelet transform to the analysis of thermograms. In [10] the PPT experiment aiming at the determination of the depth of damage with the use Artificial Neural Networks was described.

3. Problem formulation

Our aim is to detect local damage zones in a structure if such damage exists. Structures are subjected to thermal excitation, inducing variation of the temperature field, which is measured at the surface of the structure. The measured response signal is subjected to a 2-D DWT. Efficiency of damage detection in homogenous and non-homogenous structures is discussed.

3.1. Heat transfer problem

Stationary and non-stationary problems are considered. Experiments are numerically simulated as solutions of initial boundary value problems

$$\left.\begin{aligned} -\operatorname{div}\mathbf{q}(\mathbf{x},t) + f &= c(\mathbf{x})\dot{T}(\mathbf{x},t) \\ \mathbf{q}(\mathbf{x},t) &= -\lambda(\mathbf{x})\cdot\nabla T(\mathbf{x},t) \end{aligned}\right\} \quad \text{on } \Omega\,, \tag{1}$$

where $\mathbf{q}$, f, c, λ are heat flux vector, heat generated per unit volume, specific heat and material conductivity matrix, respectively. A dot above a symbol denotes the time derivative, T is temperature field and h is the convection (film) coefficient. Structure domain Ω is bounded by the external boundary Γ. On the boundary portion Γ_T, Γ_q, Γ_h the Dirichlet, Neumann and Henkel boundary conditions are specified, respectively,

$$\begin{cases} T(\mathbf{x},t) = T^0(\mathbf{x},t) & \text{on } \Gamma_T\,, \\ q_n(\mathbf{x},t) = q_n^0(\mathbf{x},t) & \text{on } \Gamma_q\,, \\ q_n(\mathbf{x},t) = h[T(\mathbf{x},t) - T_\infty(\mathbf{x},t)] & \text{on } \Gamma_h\,, \\ T(\mathbf{x},0) = T_0(\mathbf{x}) & \text{in } \Omega\cup\Gamma\,. \end{cases} \tag{2}$$

In the steady-state problem the term $c(\mathbf{x})\dot{T}(\mathbf{x},t)$ in Eq. (1) vanishes and the initial condition need not be specified in Eq. (2). It is assumed that the temperature of the environment is $T_\infty(\mathbf{x},t) = 20°\mathrm{C}$. Convection film coefficient, composing of convection and radiation parts $h = h_k + h_r$, was evaluated basing on the assumption that there is no transport of the air mass around the specimen. The convectional part h_k was computed using Grashof and Nusselt criteria and the radiation part h_r was computed assuming that the surface emission factor $\epsilon = 0.85$.

3.2. 2-D wavelet transform

In real experiments, for the purpose of defect localization, the structural response in the form of a 2-D temperature field is measured and next subjected to 2-D wavelet analysis. It allows exhibiting of local features of the signal. The background of one-dimensional discrete wavelet transform was presented in Part I. A two-dimensional wavelet transform provides a multiresolution decomposition of any 2-D signal $F(x,y) \in \mathbf{L}^2(\mathbf{R})$, which can be expressed in $3J+1$ functions, where J is the integer representing the level of wavelet transform:

$$F(x,y) = S_J(x,y) + \sum_{j=1}^{J} D_j^V(x,y) + \sum_{j=1}^{J} D_j^H(x,y) + \sum_{j=1}^{J} D_j^D(x,y)\,. \tag{3}$$

The functions S_J, D_j^V, D_j^H and D_j^D are known as the smooth image, vertical, horizontal and diagonal images, respectively. The integer j indicates the level of signal component and it is called

a scale level. In this study the orthogonal Daubechies and Haar wavelets are used. The Daubechies wavelets are compactly supported and strongly non-symmetric. They are very efficient in approximation of constant and linear functions. Haar wavelet has the simplest square form. It is the unique orthogonal wavelet, which is symmetric.

3.3. Homogeneous structures

The first part of the paper takes up the problem of damage identification in homogeneous structures subjected to stationary and non-stationary heat flux. The plate structure, schematically presented in Fig. 1a, is numerically modeled as a 2D or 3D structure. The influence of damage extent, shape and localization and also the influence of boundary conditions of thermal excitation on the effectiveness of identification is analyzed. Regular and irregular shapes of plates were assumed. To account for measurement errors a white noise is superposed on the numerical results following from Eqs. (1) and (2). Different forms of damage are considered, namely an inclusion of different material or a void localized inside the structure.

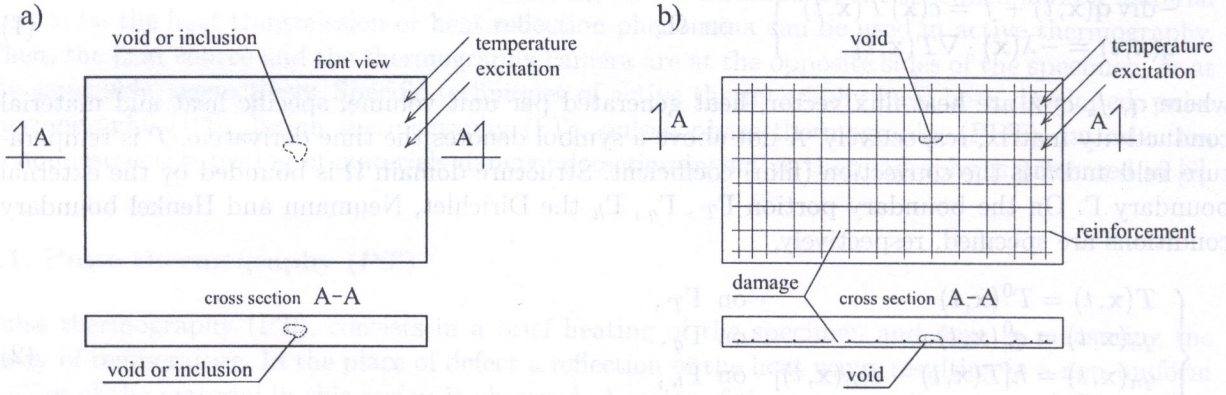

Fig. 1. Models of the thermally loaded plates: a) homogenous, b) non-homogenous

3.4. Non-homogeneous structures

The second part of the paper concerns the problem of damage detection in non-homogeneous structures. As an example, a reinforced concrete plate is considered (Fig. 1b). The plate will be subjected to various forms of thermal excitation. We will study if wavelet transform allows proper damage localization also in the case when disturbances induced by reinforcement are expected. Selection the proper type of wavelet, proper detail of scale level and detail image component will be discussed, too. Damage is assumed in the form of a gap in reinforcement bar or a void in concrete.

4. Numerical analysis

4.1. Damage detection in homogeneous structures

Henceforth we assume the initial condition $(2)_4$ in the form $T_0(\mathbf{x}) = 20°\mathrm{C}$. The Dirichlet boundary condition $(2)_1$ will be assumed as constant temperatures specified for respective surfaces, shown in Fig. 2. We will consider two types of computer simulated experiments, namely transient heat transfer and steady-state problem. In the former one the time integration is performed starting from $t = t_0$.

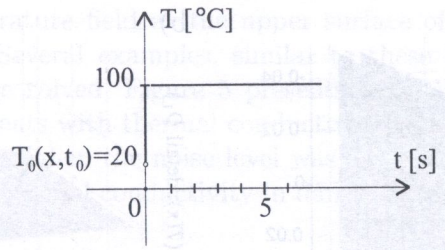

Fig. 2. Thermal excitation of plate structure

Example 1

Let us study the effectiveness of wavelet transform for various thermal excitations in cases when the defect is hidden inside the plate. Therefore, in numerical simulation of thermal experiments we will divide the plate into tree layers and use 3D elements FEM. The material parameters are as follows: density $\varrho = 7850$ kg/m^3, thermal conductivity $\lambda = 50$ W/(mK), film coefficient $h = 8.21$ W/(m^{2}K) and specific heat $c = 450$ J/(kgK). The dimensions of the plate are 12.6×6.2×0.6 cm.

Let the defect be limited to the interior layer of the plate (Fig. 3a) and let it has the form of an inclusion of different material with reduced conductivity factor.

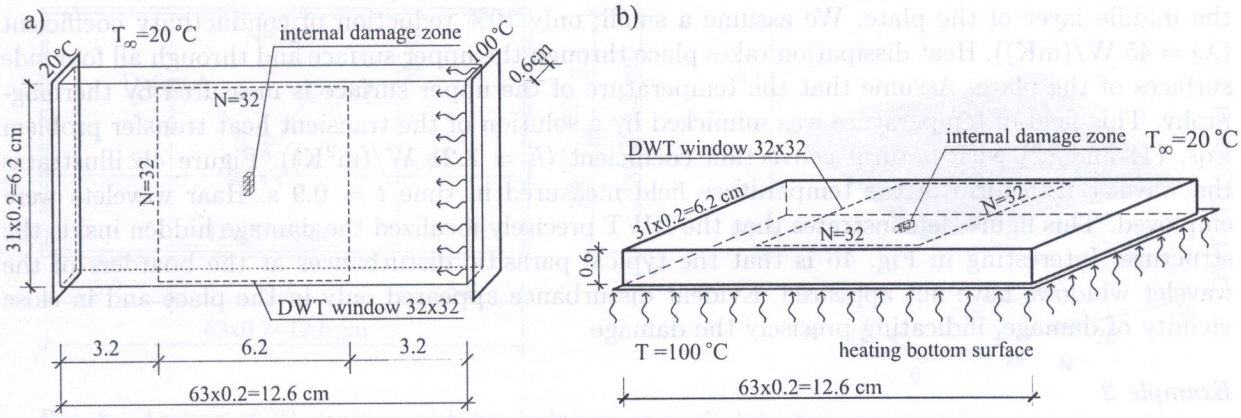

Fig. 3. Models of thermally loaded and defected plate structure: a) in-plane heat flux direction, b) transverse heat flux direction

Assume prescribed constant temperatures at the left and right edges 100°C and 20°C, respectively. Hence, the in-plane heat flux is induced. Numerical analyses proved that using DWT it was possible to detect the inclusion of different material even when its extent was as small as one FEM element (0.2×0.2×0.2 cm) located in the middle layer of the plate, provided that the reduction of conductivity coefficient was greater than 25% ($\lambda_d = 37.5$ W/(mK)). In this series of examples a steady-state heat flux was considered and the natural convection at the plate face was neglected ($h = 0$ W/(m^{2}K)).

Note, that the temperature field was recorded at the external surface of plate. Worse effectiveness of detection of the interior inclusion was observed, when problems of transient heat flux were considered, accounting for natural convection at the exterior surfaces of plate ($h = 8.21$ W/(m^{2}K)). Satisfactory detection was observed, when the size of inclusion was increased to 3 finite elements (0.6×0.2×0.2 cm) and the conductivity coefficient reduced by 50% ($\lambda_d = 25$ W/(mK)). This case is illustrated in Fig. 4a, where the DWT transform of the temperature field is presented. The wavelet Daubechies 6 was used. The temperature was measured at the moment $t = 75.50$ s.

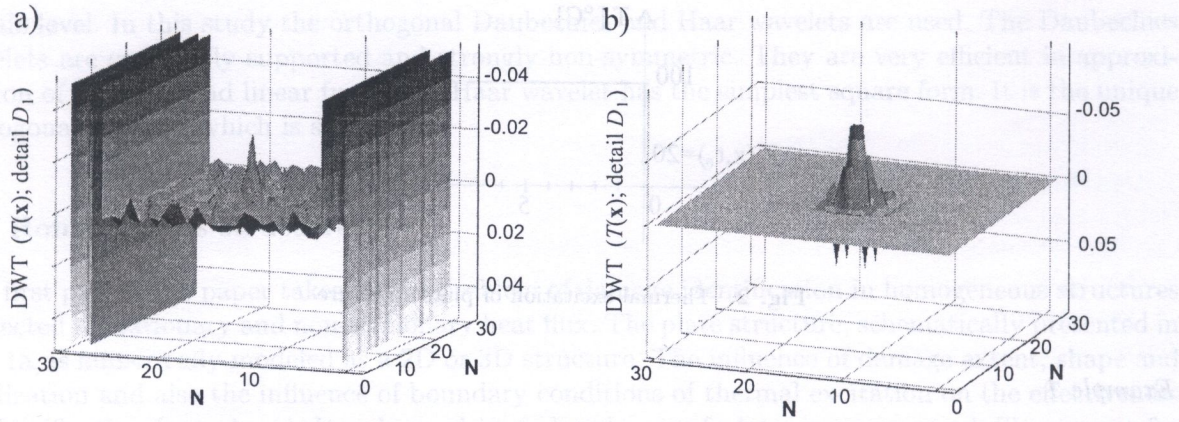

Fig. 4. DWT of temperature field in transient problem of heat transfer (h = 8.21 W/m^{2}K); number of measurement points $N = 32 \times 32$ in cases: a) in-plain heat flux, λ_d = 25 W/mK (Daubechies 6 wavelet), b) transverse heat flux, λ_d = 45 W/mK (Haar wavelet)

Example 2

Looking for the improvement of the effectiveness of damage detection we modified the last example. Consider now a horizontal plate and the constant boundary temperature 100°C at the bottom surface of the plate, shown in Fig. 3b. Hence, the transversal heat flux is induced. Let the size and location of the damaged zone be similar as in the previous example, i.e. 3 FEM size, located in the middle layer of the plate. We assume a small, only 10% reduction of conductivity coefficient (λ_d = 45 W/(mK)). Heat dissipation takes place through the upper surface and through all four side surfaces of the plate. Assume that the temperature of the upper surface is measured by thermography. This field of temperature was mimicked by a solution of the transient heat transfer problem Eqs. (1) and (2) with natural convection coefficient (h = 8.21 W/(m^{2}K)). Figure 4b illustrates the wavelet transform of the temperature field measured in time t = 0.9 s. Haar wavelets were employed. This figure demonstrates that the DWT precisely localized the damage hidden inside the structure. Interesting in Fig. 4b is that the typical parasitic disturbances at the boarders of the wavelet windows have not appeared. Evident disturbance appeared only in the place and in close vicinity of damage, indicating precisely the damage.

Example 3

Now, let us study the effectiveness of damage detection in real life situations, when inevitable errors in temperature measurements appear. We will mimic inaccurate temperature fields by the addition

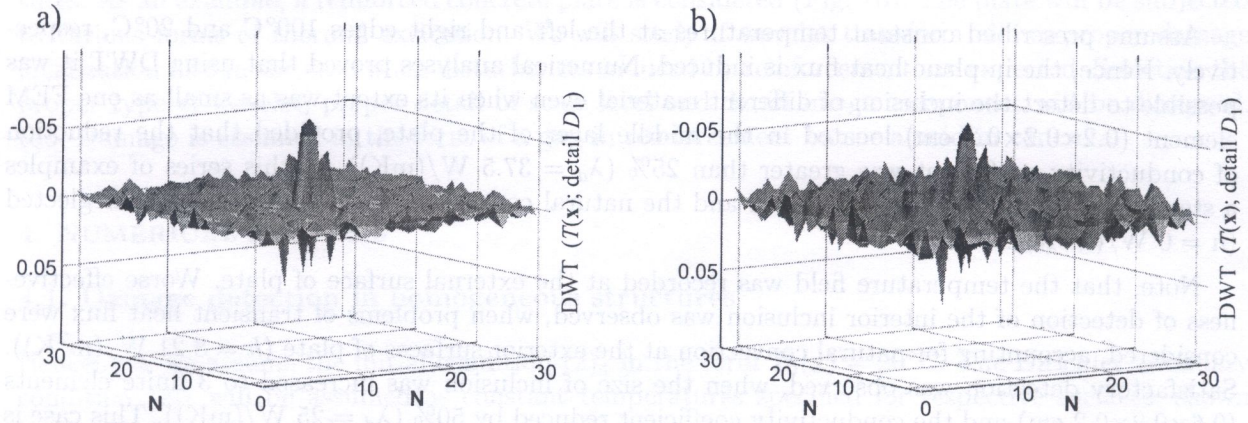

Fig. 5. DWT of temperature field with a white noise; $N = 32 \times 32$: a) level of white noise ±0.01°C, b) level of white noise ±0.02°C

of a white noise to the temperature field at the upper surface of the plate, obtained from FEM solution of Eqs. (1) and (2). Several examples, similar to these illustrated in Fig. 3b, but with variable intensity of noise were solved. Figure 5 presents the DWT when the damage was very small. It occupied 3 FEM elements with thermal conductivity reduction by 10%. In this case DWT effectively detected the damage, when the noise level was not greater than ± 0.02°C (see Fig. 5b). In case of greater reduction of thermal conductivity in damage zone, detection was possible also for higher noise level.

Example 4

Let us check now if DWT detects two or more defects existing in a small distance. Consider a plate shown in Fig. 3b with two inclusions (Fig. 6a). Each defect occupies a two-element region. The distance between defects is only 0.6 cm. Assume the thermal conductivity coefficients in defects A and B to be equal to $\lambda_d = 45$ W/(mK) and $\lambda_d = 37.5$ W/(mK), respectively. Consider an experiment with transverse heat flux. Let the temperature of one surface of the plate be 100°C and assume that the temperature is measured at the opposite surface. We consider a transient heat transfer problem allowing for natural convention ($h = 8.21$ W/(m^{2}K)). Figure 6b shows the 2D wavelet transform of the temperature signal measured in time $t = 0.9$ s. We observe evident disturbances in the detail D_1 in the places of defects A and B. Note that the disturbance connected with defect B is greater

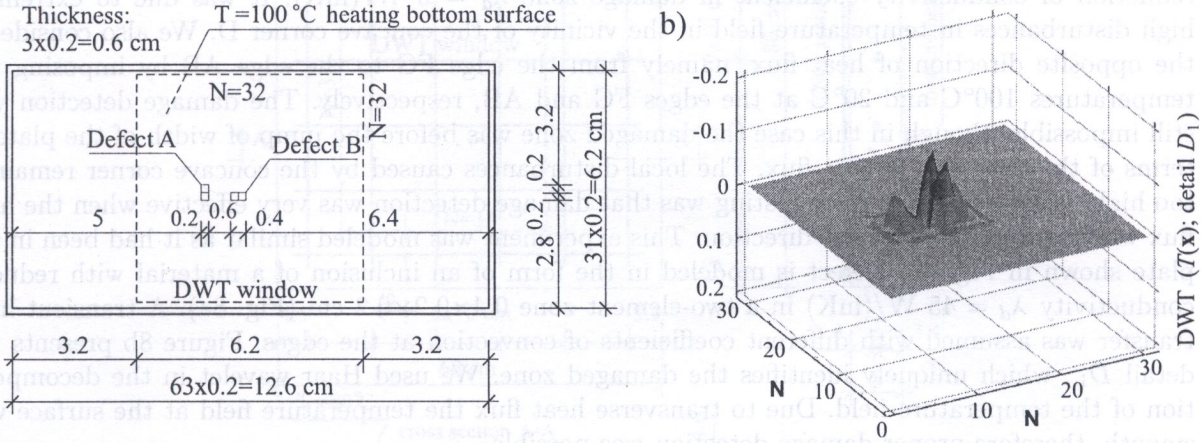

Fig. 6. Analysis of 3D structure with two inclusions at small distance in transient heat transfer problem ($h = 8.21$ W/(m^{2}K)); $N = 32 \times 32$: a) position of two inclusions at small distance, b) DWT of temperature field

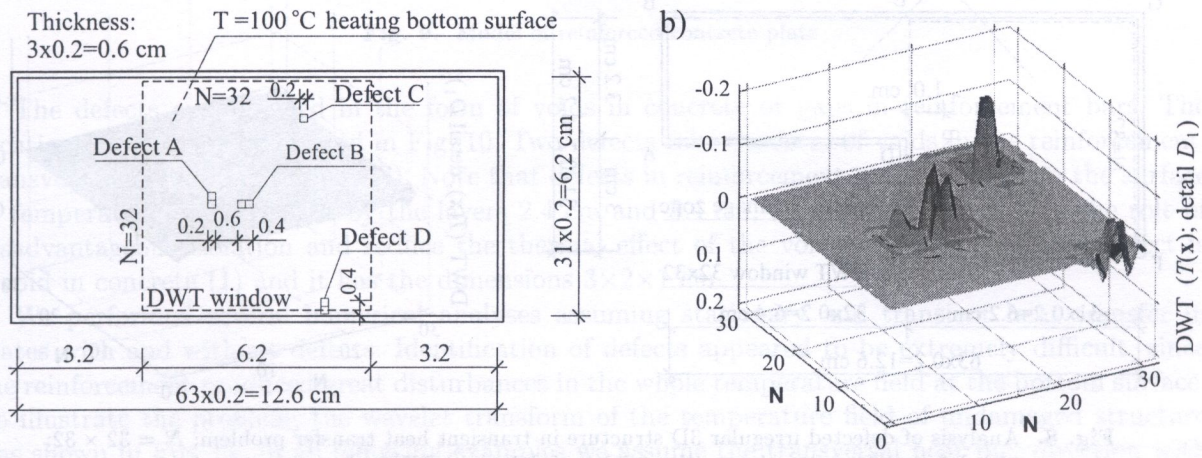

Fig. 7. Analysis of 3D structure with four inclusions in transient heat transfer problem ($h = 8.21$ W/(m^{2}K)); $N = 32 \times 32$: a) position of four inclusions, b) DWT of temperature field

than the disturbance in the place of defect A. This is in agreement with the intensity of reduction of coefficients λ_d in both defects. It proves that DWT can effectively detect two defects located close to each other and can provide information on the intensity of each defect. We used Haar wavelet.

Consider again the above discussed plate, but with two additional inclusions of material (points C and D in Fig. 7a) with reduced conductivity coefficients $\lambda_d = 25$ W/(mK) and $\lambda_d = 45$ W/(mK), respectively. Let the plate be subjected to the same heat transfer experiment as described above. Figure 7b shows the 2D wavelet transform of the temperature signal measured in time $t = 0.9$ s. The transform clearly indicates all four damage zones.

Example 5

In the following we will study the influence of irregular shape on the effectiveness of damage detection. Consider a plate shown in Fig. 8a. The internal structure of the plate is similar as it was in the plate shown in Fig. 3a. In order to check if the concave corner of the plate disturbs wavelet transforms we consider an experiment, when the right edge of plate is heated to the temperature level 100°C. Hence, the heat flux direction is from the edge AB to the section DE and further to the edge FG, where the temperature $T = 20$°C is imposed. Let the defect be located in the vicinity of the concave corner of the plate, at the distance 0.2 cm. Assume the shape of defect equal to two elements, i.e. 0.4×0.2×0.2 cm. Our attempts at damage localization failed even in case of drastic reduction of conductivity coefficient in damage zone $\lambda_d = 0$ W/(mK). It was due to extremely high disturbances in temperature field in the vicinity of the concave corner D. We also considered the opposite direction of heat flux, namely from the edge FG to the edge AB by imposing the temperatures 100°C and 20°C at the edges FG and AB, respectively. The damage detection was still impossible, though in this case the damaged zone was before the jump of width of the plate in terms of the direction of heat flux. The local disturbances caused by the concave corner remained too high. Expected and yet interesting was that damage detection was very effective when the heat flux was induced in transverse direction. This experiment was modeled similar as it had been in the plate shown in Fig. 3b. Defect is modeled in the form of an inclusion of a material with reduced conductivity $\lambda_d = 45$ W/(mK) in a two-element zone 0.4×0.2×0.2 cm (Fig. 8a). A transient heat transfer was assumed with different coefficients of convection at the edges. Figure 8b presents the detail D_1, which uniquely identifies the damaged zone. We used Haar wavelet in the decomposition of the temperature field. Due to transverse heat flux the temperature field at the surface was smooth, therefore proper damage detection was possible.

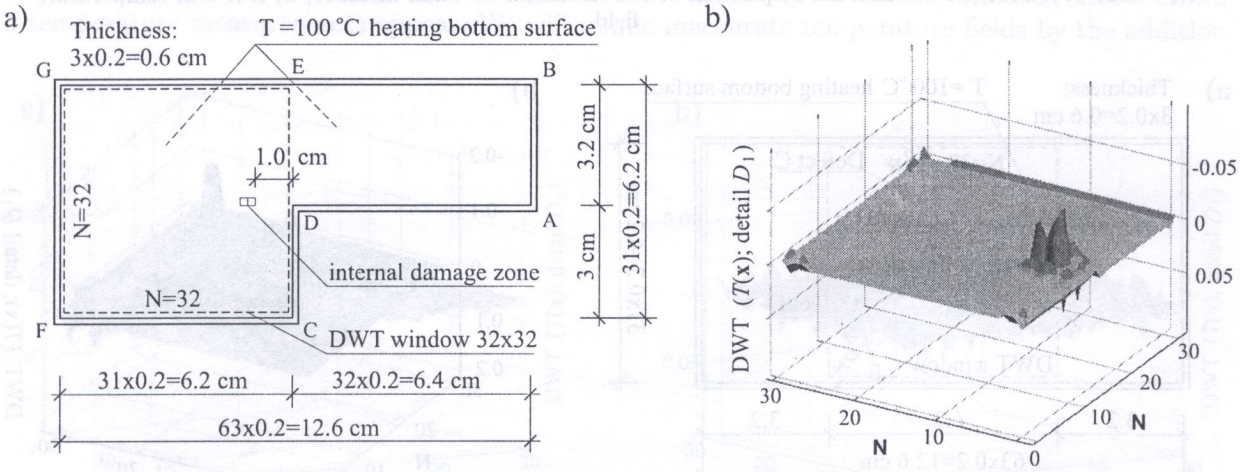

Fig. 8. Analysis of defected irregular 3D structure in transient heat transfer problem; $N = 32 \times 32$: a) defected irregular plate with position of defect, b) DWT of temperature field

4.2. Damage detection in non-homogeneous structures

A new class of problems is faced when the structure is non-homogeneous, since the disturbances of the signal can be generated both, by jumps of material parameters and by defects. We will study this issue by the way of an example of a reinforced concrete (RC) plate. Consider a RC plate 80×60×8 cm, shown in Fig. 9. The FEM mesh was generated introducing seven layers: 1×1.6 cm, 5×1 cm and 1×1.4 cm, respectively from the upper surface to the bottom one. The parameters of concrete are: density $\varrho = 2400$ kg/m^3, thermal conductivity $\lambda = 4$ W/(mK), specific heat $c = 1050$ J/(kgK), and for steel: $\varrho = 7850$ kg/m^3, $\lambda = 50$ W/(mK), $c = 450$ J/(kgK). In numerical model we neglect thermo-mechanical coupling and local effects in the interface between steel and concrete.

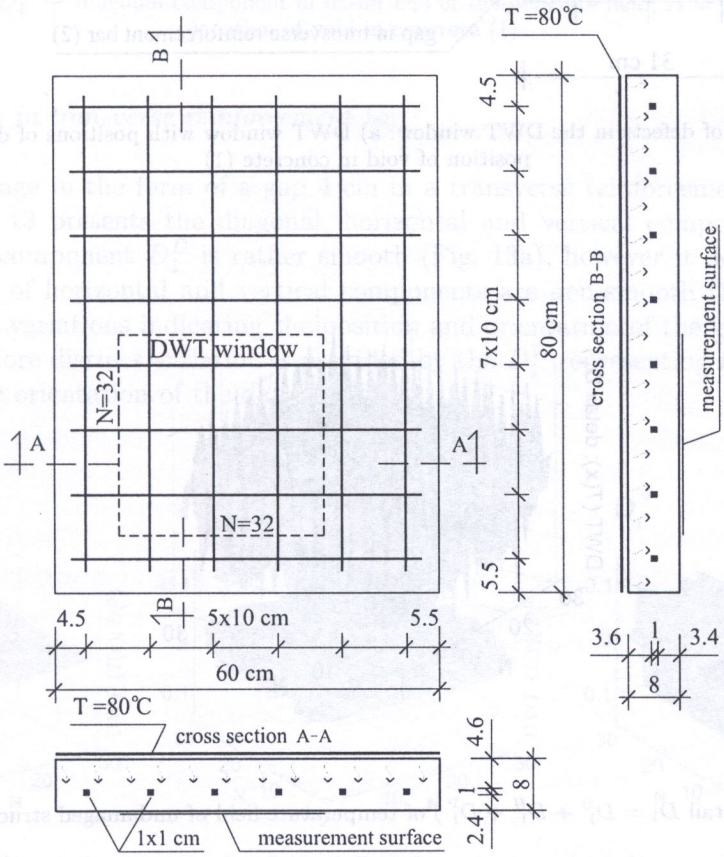

Fig. 9. Model of reinforced concrete plate

The defects are modeled in the form of voids in concrete or gaps in reinforcement bars. The location of defects is illustrated in Fig. 10. Two defects take the form of voids in the reinforcement: transverse (2) and longitudinal (3). Note that defects in reinforcement are isolated from the surface of temperature measurement by the layers 2.4 cm and 3.4 cm, respectively, which play the role of disadvantageous isolation and reduce the thermal effect of the voids in steel. The third defect is a void in concrete (1) and it has the dimensions 3×2×1 cm.

We performed several numerical analyses assuming stationary and transient heat transfer in plates with and without defects. Identification of defects appeared to be extremely difficult, since the reinforcement produced great disturbances in the whole temperature field at the bottom surface. To illustrate the problem, the wavelet transform of the temperature field of undamaged structure was shown in Fig. 11. In all following examples we assume the transversal heat flux direction with natural convection coefficient $h = 6.07$ W/(m^{2}K), and the temperature was measured for $t = 1035$ s. For decomposition of temperature signal Haar wavelet were employed.

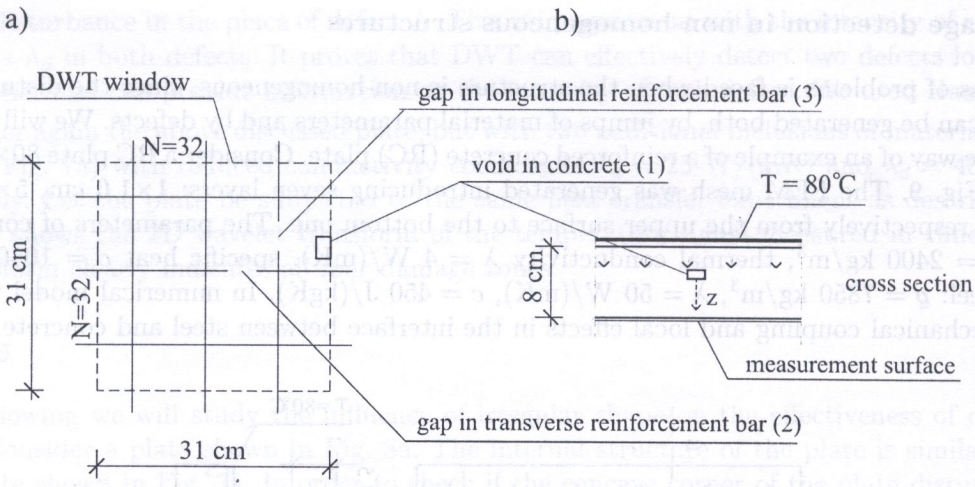

Fig. 10. Position of defects in the DWT window: a) DWT window with positions of defects, b) variable position of void in concrete (1)

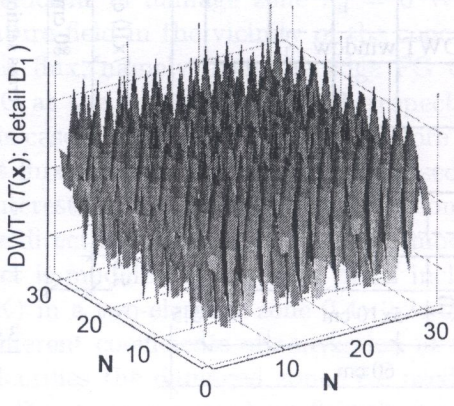

Fig. 11. DWT (detail $D_1 = D_1^D + D_1^H + D_1^V$) of temperature field of undamaged structure; $N = 32 \times 32$

Example 6.1 Damage in concrete

In this example detection of voids in concrete will be considered for various void dimensions and locations within the thickness of plate. Independent on the dimensions and location of a void, the wavelet transform demonstrated great disturbances in the whole window, similarly as shown in Fig. 11. Damage detection was not possible. Therefore we decided to study the characteristic features of vertical, horizontal and diagonal components of the detail one. It appeared that horizontal and vertical components were useless for damage detection, because they provided variations similar to these shown in Fig. 11.

Interesting is that only the diagonal component D_1 of the transform provided smooth image, which was free from disturbances caused by reinforcement (Fig. 12). Note that the range of the abscissa in Fig. 12 is $(-0.05, +0.05)$, whereas in Fig. 11 is $(-0.15, +0.15)$. Smooth image of diagonal component probably results from the fact that the reinforcement was orthogonal. Thus, the detail D_1^D demonstrated good efficiency in detection of a void 3×2×1 cm, however only for the cases when the center of the void was not deeper than 2.4 cm (Figs. 12b,c).

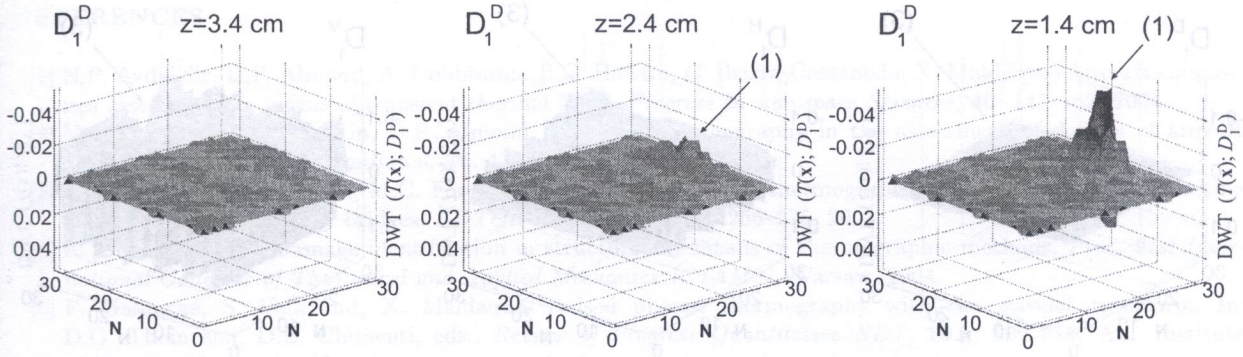

Fig. 12. DWT (D_1^D — diagonal component of detail D_1) of temperature field; $N = 32 \times 32$. Variable location of void in concrete (1)

Example 6.2 Damage in transverse reinforcement bar

Consider now a damage in the form of a gap 4 cm in a transverse reinforcement bar (damage (2) in Fig. 10a). Figure 13 presents the diagonal, horizontal and vertical components of detail D_1. Again, the diagonal component D_1^D is rather smooth (Fig. 13a), however it does not indicate the damage. The images of horizontal and vertical components are non-smooth (Fig. 13b,c), but one can notice additional variations indicating the position and orientation of the gap in the transverse reinforcement bar. More distinct variation is provided by the D_1^V representing the transform in the same direction as the orientation of the damage.

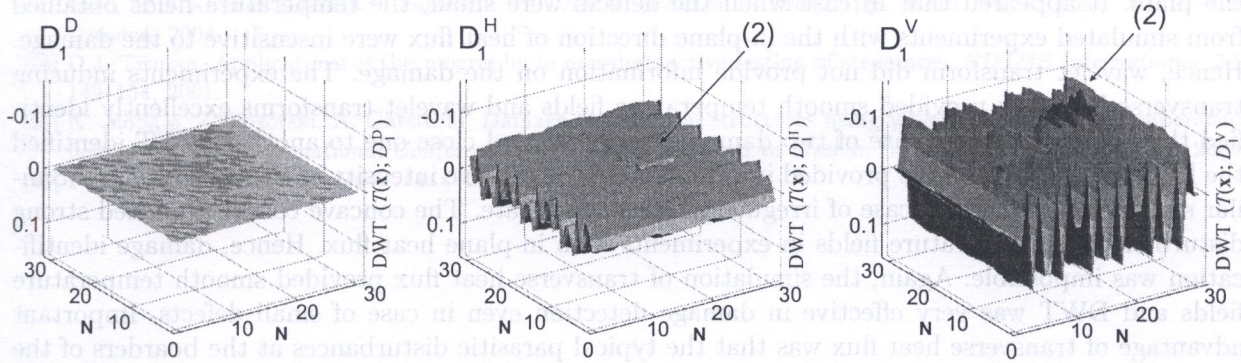

Fig. 13. DWT (respective components of detail D_1) of temperature field; $N = 32 \times 32$. Damage in transverse reinforcement bar (2)

Example 6.3 Damage in longitudinal reinforcement bar

Next consider the gap 4 cm in the longitudinal reinforcement bar (damage (3) in Fig. 10a). The results of wavelet analyses are shown in Fig. 14. They are similar to these shown in Fig. 13. This time the horizontal component D_1^H was collinear with damage orientation and therefore it better indicated the damage.

The examples 6.1, 6.2 and 6.3 demonstrate that the damage detection in non-homogenous structures is more difficult than in homogenous ones, because the response signal and the transformed signal are perturbed by both, inhomogeneous material and by damage. Nevertheless, the analysis of specific details and components of the transform provides information on the existence and orientation of damaged area.

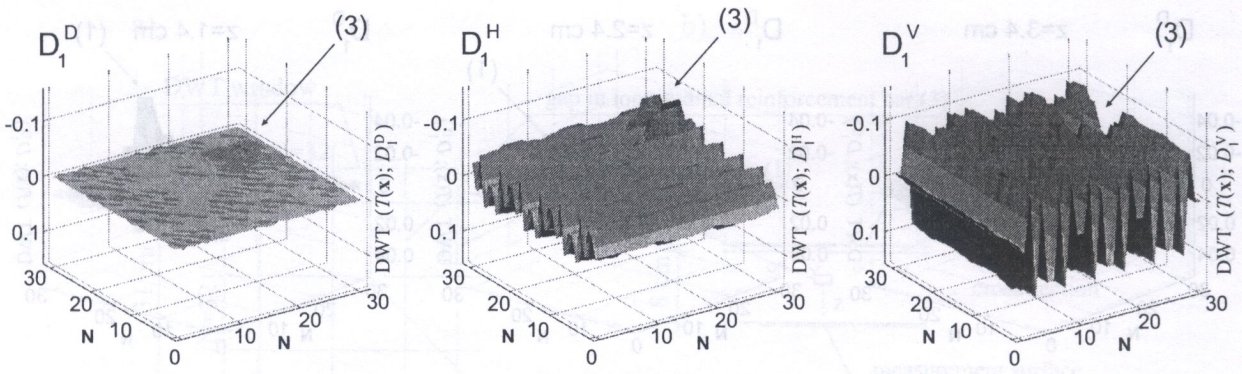

Fig. 14. DWT (respective components of detail D_1) of temperature field; $N = 32 \times 32$. Damage in longitudinal reinforcement bar (3)

5. Concluding remarks

Effectiveness of Discrete Wavelet Transform in damage identification was studied by the way of a number of examples, which referred to the temperature measurements in steady-state and transient heat transfer. Two dimensional DWT with Daubechies and Haar wavelets were used. Both types of wavelets are numerically efficient due to their orthogonality.

All examples referred to plate structures. Various types of thermal experiments were considered. Natural convection was allowed for or neglected. The heat flux was induced in the in-plane direction of the plate or in the transverse direction. Experimental results were mimicked by FEM analyses.

A series of examples discussed in the paper referred to the case when defects were hidden inside the plate. It appeared that in case when the defects were small, the temperature fields obtained from simulated experiments with the in-plane direction of heat flux were insensitive to the damage. Hence, wavelet transform did not provide information on the damage. The experiments inducing transverse heat flux provided smooth temperature fields and wavelet transforms excellently identified the damage. Even in case of two damaged zones located close one to another, DWT identified the location of damages and provided information on the relative intensity of these two defects. Similar situation was faced in case of irregular shape of the plate. The concave corner produced strong disturbances in temperature fields in experiments with in-plane heat flux. Hence, damage identification was impossible. Again, the simulation of transverse heat flux provided smooth temperature fields and DWT was very effective in damage detection even in case of small defects. Important advantage of transverse heat flux was that the typical parasitic disturbances at the boarders of the wavelet windows have not appeared.

Interesting observation was that Daubechies wavelets were more effective than Haar ones in case of in-plane heat flux and conversely, Haar wavelets proved to be more effective in case of transverse heat flux. However, the examples demonstrated that there is no general rule which type of wavelet is better.

By the way of several examples we can conclude that 2D wavelet transform can effectively detect damage even in case of small damage intensity. Unfortunately, damage detection in a structure made of non-homogeneous material is much more difficult. Jumps of material parameters at the boundaries of different materials produce many local disturbances in temperature fields. This problem needs further studies.

Acknowledgments

Financial support by Poznań University of Technology grant DS 11–657/05 is kindly acknowledged.

REFERENCES

[1] N.P. Avdelidis, D.P. Almond, A. Dobbinson, B.C. Hawtin, C. Ibarra-Castanedo, X. Maldaque, Aircraft composites assessment by means of transient thermal NDT. *Progress in Aerospace Sciences*, **40**: 143–162, 2004.

[2] N.P. Avdelidis, B.C. Hawtin, D.P. Almond, Transient thermography in the assessment of defects of aircraft composites. *NDT&E International*, **36**: 433–439, 2003.

[3] M.R. Clark, D.M. McCann, M.C. Forde, Applications of infrared thermography to the non-destructive testing of concrete and masonary bridges. *NDT&E International*, **36**: 256–275, 2003.

[4] K. Dems, Z. Mróz, Damage identification in structures by means of thermographic methods. *Proc. 21st International Congress of Theoretical and Applied Mechanics ICTAM04*, Warsaw, 2004.

[5] F. Galmiche, S. Vallerand, X. Maldaque, Pulsed phased thermography with the wavelet transform. In: D.O. Thompson, D.E. Chimenti, eds., *Review of Progress Quantitative NDT*, **19A**: 609–615, Am. Institute of Physics, Montreal, 2000.

[6] G. Giorleo, C. Meola, Comparison between pulsed and modulated thermography in glass-epoxy laminates. *NDT&E International*, **35**: 287–292, 2002.

[7] C. Ibarra-Castanedo, F. Galmiche, A. Darabi, M. Pilla, A. Ziadi, S. Vallerand, J.-F. Pelletier, , Thermographic nondestructive evaluation: overview of recent progress. In: X. Maldaque, A. Rozlosnik, eds., *SPIE Proc. Thermosense XXV*, **5073**: 450–459, Society of Photo-Optical Instrumentation Engineers, Orlando, 2003.

[8] X. Maldaque, Introduction to NDT by Active Infrared Thermography. *Materials Evaluation*, **6**(9): 1060–1073, 2002.

[9] X. Maldaque, F. Galmiche, A. Ziadi, Advances in pulsed phase thermography. *Infrared Physics and Technology*, **43**: 175–181, 2002.

[10] X. Maldaque, Y. Largouet, J.-P. Couturier, A study of defect depth using neural networks in pulsed phase thermography: modeling, noise, experiments. *Revue Generale de Thermique*, **37**: 704–717, 1998.

[11] Z. Mróz, K. Dems, Application of thermographic methods in defect identification within solid body. *Proc. 34th Solid Mechanics Conference*, Zakopane, 2002.

[12] Z. Mróz, K. Dems, Application of thermographic methods in identification of structure properties. *Proc. WCSMO-5 World Congress of Structural and Multidisciplinary Optimization*, Lido di Jesolo, 2003.

[13] Z. Pozorski, K. Ziopaja, Damage identification by wavelet transformation of data measured in thermal processes. *Proc. 75th Annual Scientific Conference — GAMM*, (PAMM — Proc. Appl. Math. Mech., eds.), **4**: 410–411, Dresden, 2004.

[14] D.J. Titman, Applications of thermography in non-destructive testing of structures. *NDT&E International*, **34**: 149–154, 2001.

[15] K. Ziopaja, Z. Pozorski, A. Garstecki, Damage detection in structures using wavelet transform of temperature field. *Proc. 16th International Conference on Computer Methods in Mechanics CMM-2005*, Czestochowa, 2005.

[16] FLIR System AB, `http://www.flir.com`.